Jonathan Beckhaus

Design of a Test Setup for Three Dimensional Indoor Positioning Systems

FAKULTÄT FÜR
INFORMATIK

Intelligent Cooperative Systems
Computational Intelligence

Design of a Test Setup for Three Dimensional Indoor Positioning Systems

Bachelor Thesis

Jonathan Beckhaus

July 16, 2019

Supervisor: Sanaz Mostaghim

Advisor: Sebastian Mai

Jonathan Beckhaus: *Design of a Test Setup for Three Dimensional Indoor Positioning Systems*
Otto-von-Guericke Universität
Intelligent Cooperative Systems
Computational Intelligence
Magdeburg, 2019.

Abstract

To implement, evaluate and calibrate indoor positioning systems, reference positions are necessary. In this thesis, a cableway as ground truth for indoor localization is evaluated. Therefore, three different methods to calculate the position of the gondola are proposed. Two of the proposed calculation approaches rely on a height sensor, built into the gondola while the third method additionally takes advantage of a motorized winch. In the end, a low cost flexible 3d ground truth with an accuracy of below 10 cm is realized.

Preface

Thank you Basti, that i could always come to you with no matter what question! Thank you Nico, Ruben and Lio for your support and your proofreading!

Contents

List of Figures

List of Tables

1 Introduction

As mobile indoor robots are getting more and more popular these days, there is also an increased need of indoor navigation and localization. Reference positions are necessary, not only to develop and improve those indoor positioning systems, but also to calibrate existing systems and determine their performance. In this thesis, a low cost 3-dimensional ground truth was built and is evaluated.

1.1 Motivation

Autonomous flight of robots is already present. Amazon for instance is about to deliver packets with drones [37]. They rely, as most of these autonomous flying drones, on GPS to get their position. Indoors however, GPS is often not an option. The Swarmlab at the Otto von Guericke University Magdeburg maintains a couple of flying indoor robots to research swarm behaviour. Next to sensors on the robots themselves, an indoor positioning solution is installed in the laboratory. To test and improve this ultra wide band localization system, a ground truth is necessary. The following section analyzes the requirements of the ground truth to improve the indoor positioning system.

1.2 Task and Requirements

The task for this work consists of the creation and evaluation of a ground truth to test indoor positioning solutions. Furthermore, a special interest is set in improving the testing of the existing ultra wide band localization system which will be used to estimate the position of drones. As a result, certain requirements need to be met.

First of all, the ground truth needs to be capable of positioning in three dimensions. Since the localization system will be used for drones, reference positions on a horizontal plane are not sufficient. Furthermore, using the same hardware for the ultra wide band localization system, "a 95 % probability positioning accuracy of 10 cm in the horizontal plane and 20 cm in the three-dimensional space was experimentally achieved" [36]. Hence, a position accuracy for the ground truth of less than 10 cm is required. Additionally, there is a cost limit of 200 euro.

The use of the ground truth also should not be limited to the installed ultra wide band localization system. Therefore, it must come with a simple setup and a high flexibility, so it can be easily installed in a different area. Thereby it can be used on different localization systems.

To be able to consider the error of the ground truth later in time, it is furthermore important to have a known error model.

A short summary of the requirements:

- test positions in three dimensions
- error of less than 10 cm
- maximum cost of 200 euro
- flexible and easy setup
- known error model

1.3 Structure of the Work

At the beginning of the work, *Basic Principles* are stated. In the *State of the Art*, existing indoor positioning systems are then compared and their use as ground truth is evaluated. After that, the *Method* of the proposed ground truth is explained. Finally, the performance of the implemented Methods is evaluated in Chapter 5. In the end, a *Conclusion* is drawn upon these results, and possible *Future Work* is shown.

2 Basic Principles

This chapter gives an overview about localization techniques used by various localization systems. Furthermore, the basic principle of two way ranging is explained.

2.1 Localization Techniques

This section summarizes the function of certain techniques used by multiple localization systems to determine a position.

Angle of Arrival

Angle of Arrival (AoA) is one of the most widely used methods for localization [27]. In this method, the angle of an arriving signal is determined [23]. Therefore, multiple receivers are installed on the tracked object. Depending on the used signal, phase shifting [23] or simply the different time the signal arrives at the different receivers is used to calculate an angle of an incoming signal (similar to binaural hearing). The anchor nodes emit an unique signal each, of which the localized object determines the angles of arrival. With the positions of the beacons known, the object can be localized [2]. It is also possible that the localized object itself emits the signal and the anchor nodes determine its angle of arrival to estimate a position.

Time Difference of Arrival

Time Difference of Arrival (TDoA) is a method used for localization, which is based on multiple synchronized anchor nodes. The object to be localized sends a signal at an unknown time. The anchor nodes then determine the different

times, the same signal arrives at each anchor nodes. With the different time of arrival for each anchor node, the position of the signal source can then be calculated. [32]

Time of Flight

Time of flight (Tof) is the time a signal travels from the sender to a receiver. While this technology is often used in depth-cameras [22], it can also be used to get a distance between two non-synchronized nodes using two way ranging [21]. With this principle, a mobile node can gather distances to various anchor nodes which can then be used to determine its position.

Received Signal Strength Indicator

The *Received Signal Strength Indicator (RSSI)* of an incoming signal can be used to approximate a distance of the receiver to the sender. This depends on the transmission power and the antenna used. The further away the sender, the smaller is the strength of the received signal. Also, the higher the frequency of the used signal, the faster the received signal strength gets attenuated over distance. Through the obtained distance to a sender, the principle of the received signal strength can be used for localization. [24]

2.2 Two Way Ranging

Through *Two Way Ranging* the time of flight of a signal can be determined. That can then be used to calculate the distance between two communicating nodes. The advantage of two way ranging is that the two nodes only need the same clock speed and no direct synchronization of its clocks. Double sided two way ranging even enables to compensate slightly different clock speeds. Figure 2.1 shows the process of double sided two way ranging between node 1 and node 2.

Node 1 registers the time it sent message A and the time it received message B to calculate the *Round Trip Time 1.* Node 2 registers the time message A arrived and the time it sent message B and sends these times within message

B. Once node 1 received message B, it can determine the *Response Time 1*. At this point, node 1 can calculate the time of flight by subtracting the *Response Time 1* from *Round Trip Time 1* and then dividing the result by two.

$$TimeOfFlight = (RoundTripTime - ResponseTime)/2$$

A single sided two way ranging would be complete by sending the resulting time of flight back to node 2 through message C. During double sided two way ranging, additionally the process to determine the *Response Time* and *Round Trip Time* is repeated for node 2 starting with message B. This way, a second time of flight is determined by node 2 and the result is sent back to node 1 with message D. In the end, both nodes have both times of flight. [34, 6, 21]

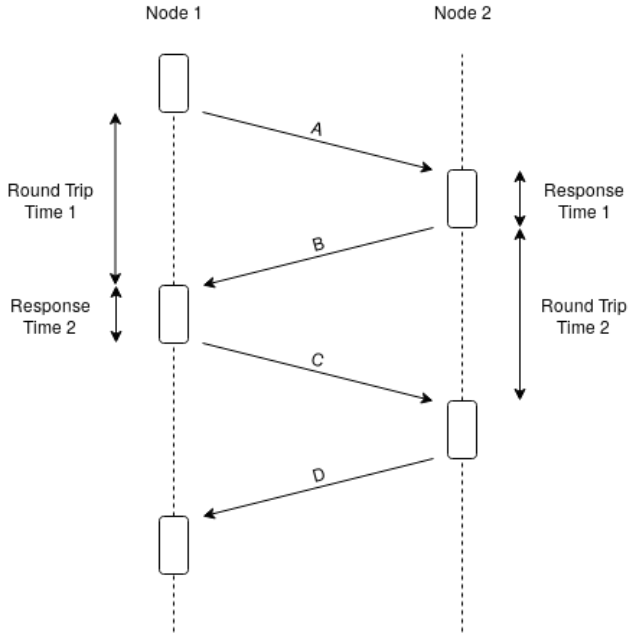

Figure 2.1: Two Way Ranging

3 State of the Art

In this chapter, existing indoor positioning systems are summarized. Furthermore their advantages and limits are shown. Eventually they are evaluated according to their use as ground truth to calibrate and evaluate other positioning systems.

3.1 Existing Indoor Positioning Systems

An indoor positioning system or indoor localization system is a system which locates objects inside buildings [26]. The position of the object is gained through different techniques such as optical [30] or radio-based [25]. This section gives an overview of existing indoor positioning systems, the way they work, their cost and other characteristics. The following structure groups these systems according to the used sensor modalities.

Wifi

Wifi is one of the most used wireless communication technologies [26] and therefore broadly available and often already installed (e.g. in an University). There are multiple ways how wifi can be used to enable localization of a wifi capable device: Time of arrival (ToA), angle of arrival (AoA), received signal strength indicator (RSSI) and combination of those [38]. Through a combination of the options named above, Yang, C. and Shao, H. [38] were able to archive an accuracy of one meter in 2-dimensional space with an estimated cost of around 200 euro using commercially available products. This enables an easy deployment of indoor navigation in buildings with already installed wifi access points, such as universities, shopping-malls or museums. Due to its low accuracy, it is not used for 3-dimensional indoor positioning but preferably used at a large scale.

Bluetooth

Like wifi, bluetooth is a widely spread technology which is supported by nearly all currently available smart phones. But unlike wifi, bluetooth infrastructure for indoor positioning is usually not already installed. Tracking and positioning with bluetooth mostly relies on the Received Signal Strength Indicator (RSSI) [15, 18, 14] of bluetooth modules. The lower the received signal strength is, the further away the mobile device is from a beacon. Using at least three beacons then enables a position estimation through triangulation in 2-dimensional space. There are commercial, (e.g. Estimote [5]) and open source solutions (e.g. AltBeacon [1]) which already implement a smart phone application and use commercially available bluetooth low energy beacons to enable a position estimation with an accuracy up to 1m in 2-dimensional space [7, 14]. Like wifi based positioning solutions, localization with bluetooth often aims to support tracking and navigation in buildings using smart phones. To estimate the cost of a minimal setup, four beacons with a price of 25 euro each [3] and a price of 100 euro for a low end bluetooth low energy capable smart phone are considered and summed up to an estimated cost of around 200 euro.

Camera Based Localization

Camera Based localization can be achieved through multiple different methods such as using depth-cameras [30], printable tracking markers [28] or using an infrared based system [19]. Depending on the needed area of position estimation, the accuracy, update rate and price, different technologies and methods can be used [30]. Commercially available systems can be set up and calibrated to an accuracy of under 1mm [8] [30] , but often cost thousands of euro. De Amici et al. [19] have been able to create an IR based 3-dimensional tracking system using Wii remote controllers and 16W IR iluminators. They used four remote controller and four iluminators to archive a mean tracking error of 1.2mm in a 12 m^3 space. The object consisted of IR reflecting markers which can be located through the WII remote controller. The cost of the used hardware is about 600 euro. General problems of camera based solutions are their complex calibration, high need for computational power and difficult setup. Additionally the costs largely scale with the space to be observed, since more cameras or cameras with higher resolutions are required.

Ultra Wide Band (UWB)

Ultra wide band communication enables the user to get a distance between two communicating nodes. This can be achieved by using the time of flight of a transmitted signal [21]. Using at least four ultra wide band communication modules as anchor nodes enables the position estimation of a fifth module in 3-dimensional space [25, 36]. Depending on the used hardware and the processing algorithm, average positioning accuracy of 56cm [25] to less than 20 cm [36] can be achieved. Tiemann et al. [36] used nine DWM1000 based modules, of which eight have been used as anchor nodes, with a cost of around 50 euro per module. This leads to an estimated cost of 450 euro for this localization system.

Ultrasonic

Ultrasonic sound can be used to locate a receiver in 2-dimensional and 3-dimensional space. This can be achieved using two different approaches. The distance between a sender and receiver can be determined by synchronizing the sender and receiver through a radio signal. Then, the position of the receiver can be calculated using multiple senders as anchors, all synchronized with the receiver [16]. The second option is to use the time of arrival (ToA) to calculate a position of the receiver and to then use the distances to the nodes. Through multiple receivers on the node which is to be tracked, with a certain distance to each other, the different time of arrival of each receiver can be used to determine an angle to the sending node which's signal has been received. Using defined time slots for each anchor node to send its signal, a position of the receiver can be determined. This approach enables an ultrasonic based tracking without synchronization [39]. In 2-dimensional space an accuracy of around 1cm can be achieved [39, 33]. According to Bjerknes et al. [16], in 3-dimensional space an accuracy below 5cm can be obtained, when properly calibrated. To approximate the setup cost, parts used by Bjerknes et al. [16] are taken as reference which results in a total costs of around 300 euro.

Multimodal Positioning

Apart from camera based self locating of a robot, robots often use a combination of sensors to locate themselves through a Simultaneous Localization

and Mapping (slam) algorithm. Such an algorithm relies on a laser scanner to obtain distances from the robot to obstacles around it. Combined with odometry information gained for example from the movement of the wheels and a gyroscope, it can generate a map of the environment and locate itself within this map [13]. A cheap robot available, capable of performing Simultaneous Localization and Mapping, is the Turtlebot with a price of 580 euro [9]. According to the datasheet of the laser scanner used by this robot [4] it has an accuracy of up to 1,5 cm. Assuming an ideal slam algorithm, the accuracy of the laser scanner can be used to approximate the 2-dimensional positioning-accuracy of the robot in a suitable indoor environment. Compared to previously mentioned methods of positioning, a self locating robot does not rely on pre-installed sensors, modules or markers and therefore can be easily placed into a different indoor environment, which makes this method of positioning very flexible.

3.2 Evaluation of Indoor Positioning Systems as Ground Truth

This section summarizes which of the shown methods above can be used as setups to evaluate and calibrate other indoor positioning systems. A ground truth for an indoor positioning system needs to have at least the maximum achievable accuracy of the indoor positioning system which is to be tested. Furthermore, the ground truth needs to provide at least the amount of dimensions of the tested system. Depending on the size of the indoor positioning system, a ground truth, to be used for calibration, either needs to have a working area big enough to cover a certain part of the indoor positioning system or needs to be flexible enough to enable an easy repositioning of the ground truth. A possible scenario could be the calibration of a wifi based navigation system in a shopping mall. This would require only 2 dimensions on each level of the building with an accuracy of about 1m in a big test environment. In Table 3.1, an evaluation of the configurations shown above can be seen. The optical indoor positioning system has the highest accuracy, but also comes with the highest price. Another drawback of such camera based systems is their typically complex setup and a rather small covered area (12 m^3 in the compared example system [19]). Wifi and bluetooth based systems come with the smallest cost but also the smallest accuracy. Furthermore they are mostly

used for 2-dimensional position estimation (as the compared example setups [7, 14, 38]). Apart from the self locating robot, the other systems introduced above require an installation and therefore are not very flexible. Using an already installed system in a different room would require much time and often a recalibration. Table 3.2 shows a rating of a systems ability to be used as a ground truth for other indoor positioning systems. Due to its high precision, the camera based position estimation can be used to evaluate and calibrate systems such as the ultra wide band and ultrasonic based localization. However, it is less appropriate for evaluating large scale indoor positioning systems such as wifi and bluetooth based setups because of its often very small operation area. Ultrasonic and ultra wide band localization methods are more easily expandable and are therefore suitable for this task. Because of the small accuracy of wifi and bluetooth based approaches they are less likely to be used as ground truth. The robot based test setup and the wifi and bluetooth based test setups chosen for the comparison in Table 3.1, only support a two dimensional indoor positioning. Those systems are capable of 3-dimensional indoor positioning which usually results in higher cost and lower accuracy.

This leaves room for a three dimensional setup which is more flexible than an ultra wide band or an ultrasonic based solution, with less calibration and setup necessary and less cost while maintaining similar accuracy. This would enable the system to also be used to evaluate and calibrate large scale wifi and bluetooth based indoor positioning systems with way lower costs.

Criteria	Camera	Robot	UWB	Ultrasonic	Wifi/Bluetooth
Dimension	3	2-3	3	3	2-3
Accuracy	<2mm	>=1,5cm	<20cm	<5cm	1m
Cost in Euro	>=600	580	400	300	200
Installation	complex	simple	complex	complex	complex
Flexibility	low	high	low	low	low
Covered Area	small	large	medium	medium	large

Table 3.1: Comparison of Possible Setups

Ground Truth	Evaluated System					
	Camera	Robot	UWB	Ultrasonic	Wifi	Bluetooth
Camera		+	++	++	-	-
Robot	- -		+	+	++	++
UWB	- -	-		-	+	+
Ultrasonic	- -	-	++		+	+
Wifi	- -	- -	- -	- -		+
Bluetooth	- -	- -	- -	- -	+	

Table 3.2: Suitability of Introduced Possible Setups as Ground Truth

4 Method

A cableway can be used as a three dimensional ground truth to analyze and calibrate other indoor positioning solutions. This chapter proposes three methods to calculate the position of the cable car.

The cableway consists of a track rope which is attached to the two anchor points P_l and P_h whereas P_l is the lower and P_h the higher mounted anchor point. A cable car (G), also named gondola, is connected to the cableway so that it can slide along the cableway. Furthermore, the cable car has a distance sensor built in looking downwards to measure its height h from the ground. The gondola is moved along the cableway by a motorized winch using a dedicated rope. The winch can determine the length of rope pulled in and therefore the distance the gondola is pulled up.

To simplify following calculations, two different coordinate systems are used. Each point of the cableway can be seen in real world coordinates (x, y, z) and in a 2-dimensional perspective (coordinates l, z). The 2-dimensional definition of a point is based on the side view of the cableway. Points on the cableway can be transferred from their 2-dimensional representation into the 3-dimensional representation by using the real-wold coordinates of the anchor points P_l and P_h of the cableway.

4.1 Linear Model

The first method is based on the assumption that the track rope, the gondola moves along, is a straight line. In Figure 4.1 the approach is shown in a two dimensional perspective with G as the gondola and P_l and P_h as anchor points. Furthermore the position of the anchor points and the distance h, measured through the distance sensor mounted on the cable car, are known.

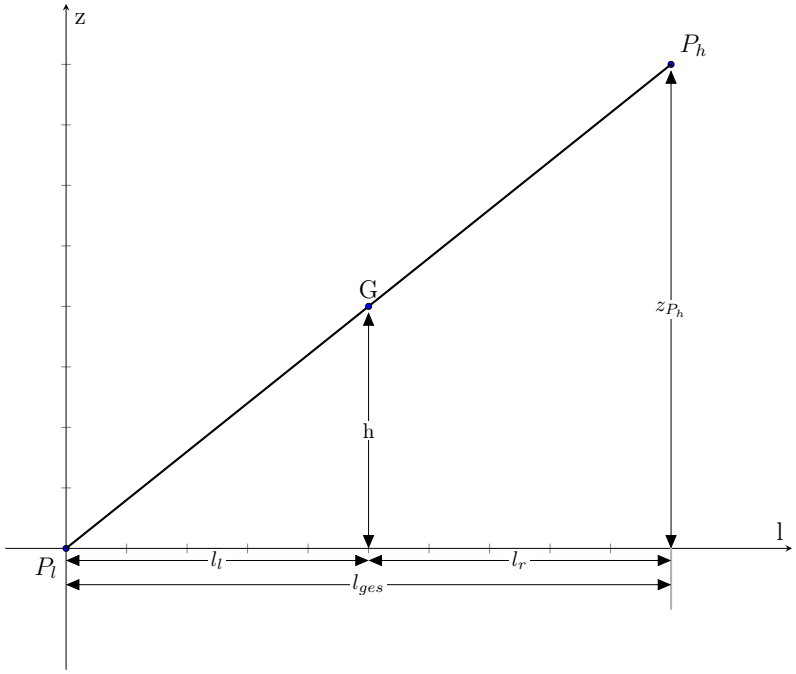

Figure 4.1: Linear Approach

To calculate the position of G, l_l and h are required (Equation 4.3). While h is already given through the height sensor, l_l can be calculated through the equal relation of z_{P_h} to h and l_{ges} to l_l (Equation 4.1, 4.2). l_{ges} is the distance of the cableway anchor-points projected to the ground and is therefore defined by their positions.

$$\frac{h}{h_{P1}} = \frac{l_l}{l_{ges}} \tag{4.1}$$

$$l_l = \frac{h}{z_{P_h}} * l_{ges} \tag{4.2}$$

$$G = (l_l, h) \tag{4.3}$$

4.2 Nonlinear Model: Step Count Method

The second method aims to compensate the slack of the cableway by approximating it with 2 straight lines, one from each anchor point (P_0 and P_1) of the

cableway to the cable car G (Figure 4.2). However, the slack d is not directly used to calculate the position of the gondola. Therefore, the rope intake of the winch pulling up the gondola, is used to calculate the distance l_t.

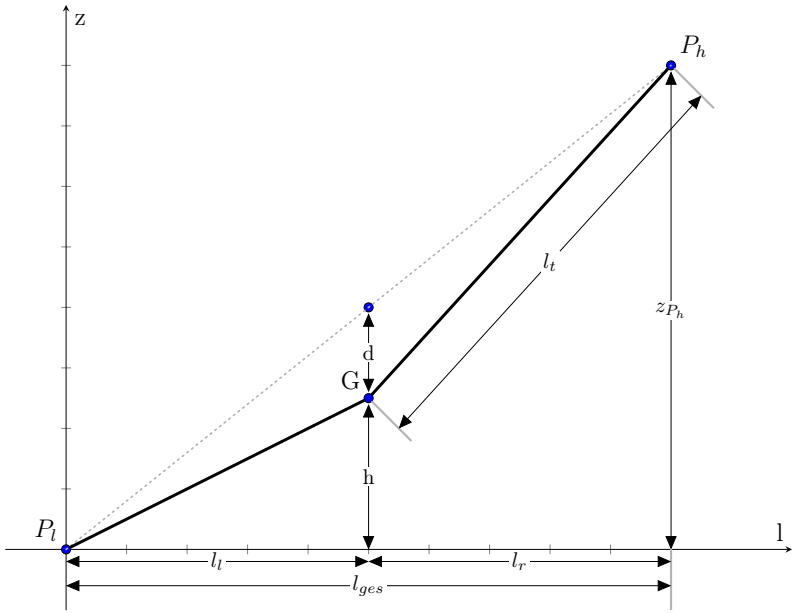

Figure 4.2: Step Count Method

Again, the positions of the anchor points, and the height h of the gondola are known. With l_t, the distance l_r can be calculated using the Pythagorean theorem (Equation 4.4). Eventually the position of G can be determined as in Equation 4.5.

$$l_r = \sqrt{l_t^2 - (z_{P_h} - h)^2} \tag{4.4}$$

$$G = (l_{ges} - l_r, h) \tag{4.5}$$

4.3 Nonlinear Model: Slack Method

In the third method, the slack of the track rope is calculated. As to see in Figure 4.3, the assumption still is that the slack d can be seen through two straight lines from the cable car G to its anchor points P_l and P_h. There

are 2 different steps to calculate the slack. First of all, the rope-tension s is determined. Therefore the slack d and the position of the cable car need to be measured. With the rope tension, the slack at any point of the cable way can then be calculated in the second step. Eventually, the resulting slack function is used to calculate a path of the gondola (dashed line in Figure 4.3). In the end, the measured height h can be used to get the position of the gondola on that path.

Calculate the Rope Tension s

In this section, the calculation of the rope tension is explained.

Next to the position of the anchor points P_l and P_h, the position of G is known. Therefore the slack d for the known position G can be calculated.

Figure 4.4 shows the cableway geometrically while Figure 4.5 represents the forces applied to the cableway and the gondola. There it can be seen that the rope tension s is defined by α and g_0 (Equation 4.11). To calculate g_0, the tangent T_l and T_r are used. They are represented in both views and represent the link between the physical and geometrical view (Equation 4.8, 4.9). Furthermore, they can be easily calculated because d and the position of G and the resulting distances l_l and l_r are known. Equation 4.12 and 4.13 are obtained by inserting Equation 4.11.

$$h_l = \tan\alpha * l_l \tag{4.6}$$

$$h_r = \tan\alpha * l_r \tag{4.7}$$

$$T_l = \frac{h_l - d}{l_l} = \frac{g_0 - g_l}{s} \tag{4.8}$$

$$T_r = \frac{d + h_r}{l_r} = \frac{g_0 + g_r}{s} \tag{4.9}$$

$$g = g_l + g_r \tag{4.10}$$

$$s = \frac{g_0}{\tan\alpha} \tag{4.11}$$

Eventually, g_l in Equation 4.12 is replaced with $g_r - g$, which results in Equation 4.14. The weight g of the gondola canceled out later, once the rope tension is used to calculate the slack. Solving Equation 4.14 and 4.13 for g_0 , Equation 4.15 is yielded. Because g_0 is canceled out, Equation 4.16 can be obtained

from Equation 4.15 so that g_r can be calculated. Finally, with g_r , g_0 can be calculated which is then used to gain the rope tension s (Equation 4.11).

$$T_l = \frac{(g_0 + g_l) * tan(\alpha)}{g_0} \tag{4.12}$$

$$T_r = \frac{(g_0 + g_r) * tan(\alpha)}{g_0} \tag{4.13}$$

$$T_l = \frac{(g_0 + g_r - g) * tan(\alpha)}{g_0} \tag{4.14}$$

$$g_0 = \frac{g_r * tan(\alpha)}{T_r - tan(\alpha)} = \frac{(g_r - g) * tan(\alpha)}{T_l - tan(\alpha)} \tag{4.15}$$

$$g_r = \frac{g(T_r - tan(\alpha))}{T_r - T_l} \tag{4.16}$$

Calculate the Slack

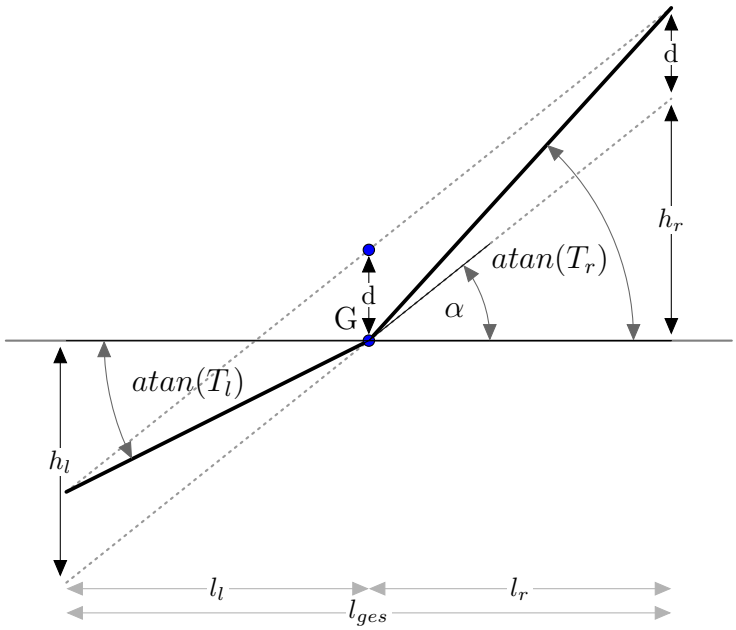

Figure 4.4: Slack Method Geometric View

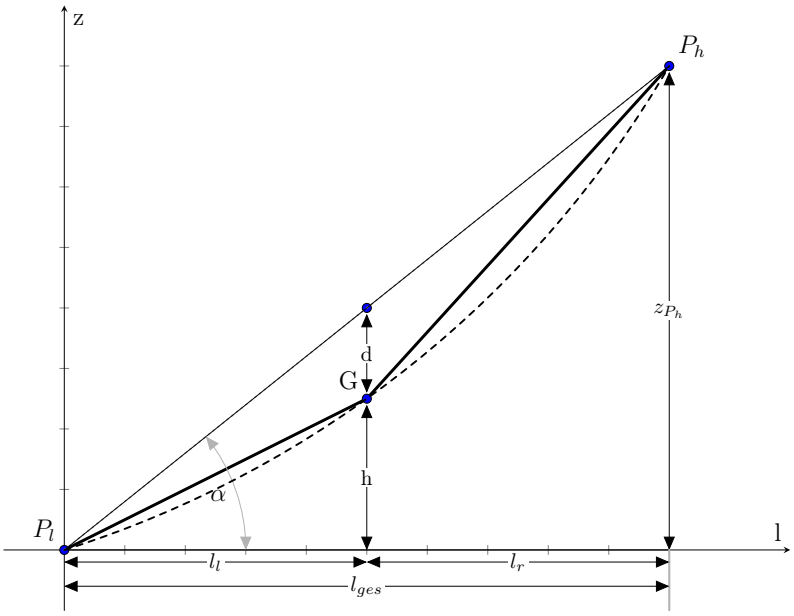

Figure 4.3: Slack Method

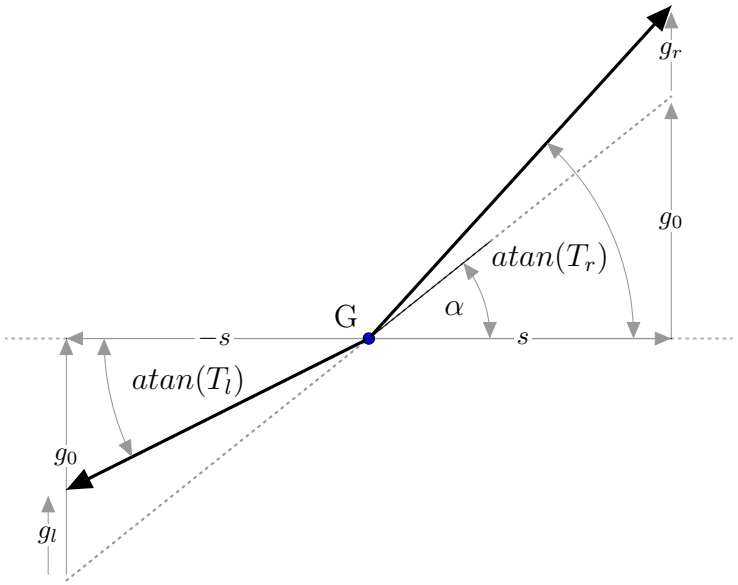

Figure 4.5: Slack Method Applied Forces

Once the rope tension s is calculated, it is used to gain the slack d. Therefore, Equation 4.8 and Equation 4.9 are used. In Equation 4.8, g_l is again replaced by $g - g_r$ (Equation 4.17). Furthermore, Equation 4.18 is solved for g_r (Equation 4.19) and then combined with Equation 4.17 to yield Equation 4.20. Eventually, Equation 4.20 is solved for d (Equation 4.21).

In the end, a slack function can be calculated with Equation 4.21. By subtracting the slack function from the linear function P_l to P_h, a path of the gondola is generated (dashed line in Figure 4.3).

To obtain a specific position for G, the measured height h is used to find the position of the gondola on the calculated path.

$$T_l = \frac{h_l - d}{l_l} = \frac{g_0 + g_r + g}{s} \tag{4.17}$$

$$T_r = \frac{d + h_r}{l_r} = \frac{g_r + g_0}{s} \tag{4.18}$$

$$g_r = \frac{(d + h_r) * s}{l_r} - g_0 \tag{4.19}$$

$$\frac{h_l - d}{l_l} = \frac{g_0 + (d + h_r) * s/l_r - g_0 + g}{s} \tag{4.20}$$

$$d = \frac{-s * h_l + h_r * (s * l_l)/l_r + g * l_l}{-s - (s * l_l)/l_r} \tag{4.21}$$

$$\tag{4.22}$$

[12]

5 Experiments and Results

In this chapter the implementation of the existing test setup and the performance of the three approaches mentioned above are described. First, the used DWM1000 ranging modules are specified, followed by the test setup and the recording of the data. After that, the methods to calculate the position of the gondola are evaluated. In the end, the installed ultra wide band localization system is considered.

5.1 DWM1000 Ranging Module

For the installed ultra wide band localization system, custom boards are used. They consist of an STM32L443CC microcontroller and a DWM1000 chip. [29] The DWM1000 chip installed on the module can communicate using a frequency of 3.5GHz - 6.5GHz [20] and is capable of time of flight measurement using two way ranging [21]. The achievable ranging accuracy of the DWM1000 chip is below 10 cm [36].

5.2 Basic Test-Setup

Variable	X	Y	Z
P_{l1}	0.110m	0.000m	0.140m
P_{l2}	-2.762m	5.261m	0.080m
P_h	4.520m	3.212m	2.630m
$A1$	0.000m	0.150m	2.999m
$A2$	4.406m	0.192m	2.999m
$A3$	0.685m	0.220m	0.115m
$A4$	0.658m	2.895m	0.125m
$A5$	4.920m	0.145m	0.220m
$A6$	4.920m	2.960m	0.220m
$A7$	4.287m	3.804m	1.154m
$A8$	-2.345m	6.005m	2.550m
$A9$	-2.073m	3.203m	2.553m

Table 5.1: Test Setup Variables

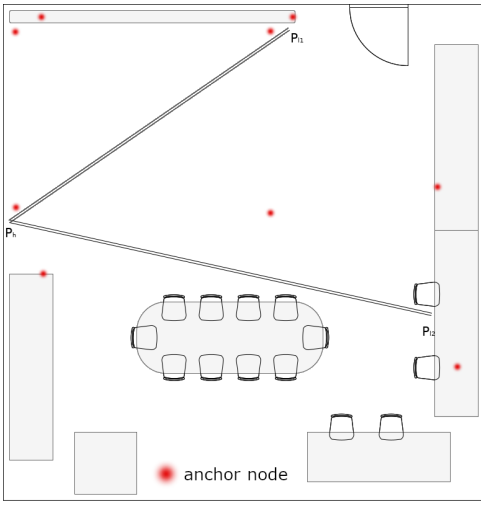

Figure 5.1: Top Down View of the Laboratory

The test setup implements a cableway mounted on two points. On the lower mounting point (P_l), a mechanism to tension the track rope was deployed. On the track rope, the cable car (or gondola) was mounted using a carabiner (Figure 5.2). The cable car itself consists of a battery, a DWM1000 module and a TeraRanger distance sensor [11], which is mounted downwards onto the gondola. Furthermore, the microcontroller on the DWM1000 module was programmed to read the height of the gondola from the distance sensor [1] two times a second. Each time a distance is measured, the DWM1000 module then broadcasts a message containing the current height. On the upper mounting point (P_h) a pulley was installed. The pulley was used to redirect the rope to pull up the cable car. The rope, used to pull up the cable car, is wound up on a stepper motor powered winch (Figure 5.3). A generic nema17 stepper motor

[1] the i2c protocol is used to read the data from the distance sensor

was used [2]. Through the ratio of the gears and the diameter of the winch, one step [3] equals a rope intake of 0.0269 mm.

In addition to the cableway, an ultra wide band based localization system was installed. Therefore, nine DWM1000 modules, A1-A9 (Table 5.1), were set up as anchor nodes. The DWM1000 module which is built onto the gondola is capable of initiating two way ranging to each anchor node in order to obtain its distance to the particular anchor node. The times generated by the two way ranging are transformed into distances using the conversion of Hempel [21]. Between each initiation, a delay of 100 ms is used to ensure a stable ranging, which results in a complete update of all distances in less than one second. To evaluate and use the data, another DWM1000 module was connected to a laptop via USB, to receive the distances from the gondola to the anchor nodes and the height of the gondola measured by the distance sensor. Additionally, commands can be sent to the DWM1000 module connected to the stepper motor to move the gondola along the cableway. The cableway was set up two times with a different lower anchor point each time. The first setup used P_{l1} and the second setup P_{l2} as lower mounting point for the cableway. Figure 5.1 shows a top-down view of the laboratory with the two different cableway setups and the installed DWM1000 anchor nodes as red dots.

5.3 Logging Procedure and Recorded Data

Two different data sets were recorded using the same procedure. The first data set is based on the first setup of the cableway with the anchor points P_h and P_{l1} whereas the second data set was generated using the cableway with P_h and P_{l2} as anchor points (Table 5.1).

To record a data set, the gondola performed one run along the corresponding cableway. Therefore, the cable car first went to a homing position. This position was determined using the height sensor. To maintain tension in the pulling rope, the gondola was only driven upwards to the positions where the data was logged. That means that the homing position was the lowest point logged. During the experiments, a homing height of 40 cm to the ground was

[2] The microcontroller on a DWM1000 module was programmed to drive the nema17 stepper motor using an a4988 stepper-driver and a c stepper library [10].

[3] The stepper motor was driven with 16th steps and has 200 steps per revolution.

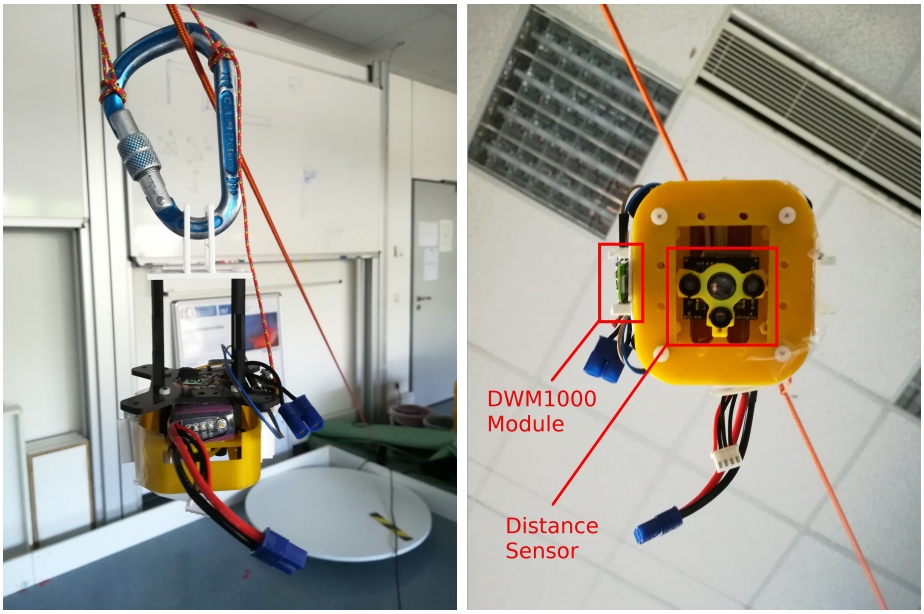

(a) Side View (b) Bottom View

Figure 5.2: The Gondola at the Cableway (Orange Rope)

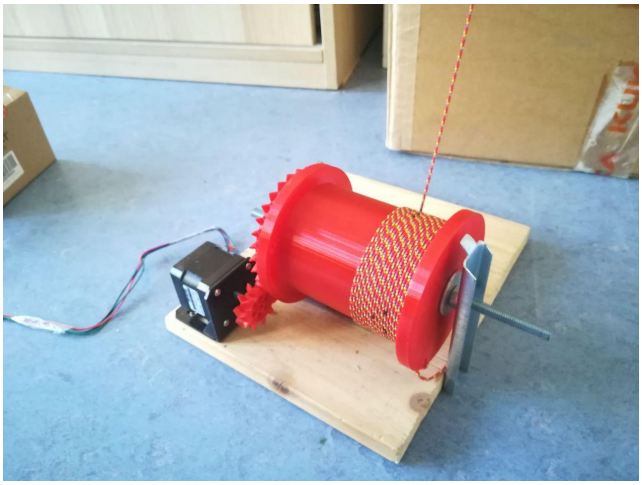

Figure 5.3: Stepper Motor Powered Winch

used. Once the position was reached, the motor based count of steps was reset to zero. Furthermore, l_{thome}, the distance from the cable car at its home position to the upper anchor point P_h, was measured at this point, once for each setup, using a laser distance measuring device [17]. l_{thome1}, with 4.598m, is the distance measured for the first data set, and l_{thome2}, with 4.48m, for the second. While the cable car was still at its home position, all data received by the DWM1000 module connected to the computer were logged 20 times with a delay of 500ms between each recording. This includes the distances from the DWM1000 module mounted on the gondola to its nine anchor nodes, its height and the step count of the motor (Table 5.2), which in this case was zero. After the recording of the 20 data samples, the gondola was moved 6000 steps upwards along the cableway, which equal around 16 cm. During the recording of the second data set, the gondola was only moved by 5000 steps (around 13.5 cm). Once the cable car has arrived, the logging of the distances, height and step count was repeated. Therefore, again, 20 data samples were taken. This procedure was repeated for 20 positions for the first and for 24 positions for the second data set. In the end, a log file with 20 times 20 entries for the first, and 24 times 20 entries for the second data set was generated.

To evaluate the calculation results generated by the three methods proposed earlier, a mark at the ground directly under the each log position of the cable car was made during both recordings. To ensure that the mark is directly under the gondola a laser-pointer was placed upright pointing at a specific point of the cable car (Figure 5.4). After the logging procedure was finished, all distances from the marks to the lower anchor point of the cableway were measured (Table 5.2). The distances equal the l value for each point of its 2-dimensional representation. With these distances and the measured height of the gondola, the 20 positions of the cable car during the first log and 24 positions during the second can be calculated and later used as reference.

Variable	Times Recorded per Position
Motor Steps	20
Measured Height	20
Ranging Distances	20
Measured Distance l	1

Table 5.2: Recorded Data per Point

Figure 5.4: Markings on the Ground for the Manual Measured Distances

5.4 Evaluation of the Homing Procedure

An essential part of the logging is the homing of the cable car. During the homing procedure the gondola is driven below a measured height of 40 cm and eventually slowly moved upwards until a height of 40 cm has been reached again. This is to ensure tension in the pulling rope. To evaluate how reliable the homing procedure is the gondola first was moved to a random position above the homing point at the cableway. After that, the homing procedure was initiated. Once the homing finished, the distance l was measured by using the same laser pointer based method as for the logging. This process was done 10 times on the first setup of the cableway.

The homing varies by a maximum of +-1 cm (Figure 5.5), with a standard deviation of 0.60928 cm. The accuracy of the homing is mainly based on the height sensor. Since the sensor's resolution is 0.5cm [35] and the ascent of the cableway is approximately 1/3, the smallest change in the distance reported by the sensor would result in a change of 1.5 cm in l_l. Further problems that can have a negative impact on the accuracy are based on the structure of the homing procedure itself. During the procedure, once the homing height is reached, the message is received by the DWM1000 module attached to the

computer, which then sends a message to the motor to stop. The wireless communication can lead to delays and thereby influence the movement. Also, the unchanged update rate of the height sensor during the home movement of two times per second and slight swinging of the gondola can affect the exact position driven to. Therefore, the results are better than originally expected.

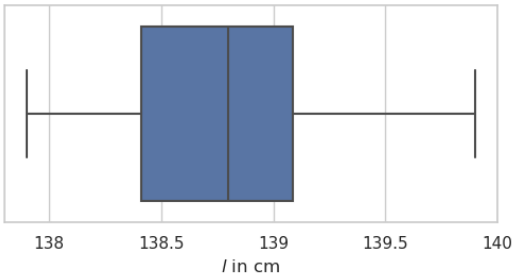

Figure 5.5: Variation of the Gondola Homing Position

5.5 Evaluation of the Linear Model

In this section, the approach of assuming that the rope is a straight line is used to calculate the position of the cable car. The calculated position of the cable car is the position where the carabiner, attached to the gondola, touched the track rope. Therefore, the height of the gondola is added up to the measured height of the distance sensor. Also, the height of the lower mounting points to which the track rope is attached to, is compensated. As a reference, the positions of the gondola are calculated by using the manually measured distances l and the mean of the measured height over the 20 values for each position. All calculations are performed on the two data sets described above. Figure 5.6 shows a 2-dimensional representation of the results compared to the reference points. The calculated positions use the mean height for each position. Therefore, the height always equals the reference. However, the calculated distance l is between 22.5 cm and 40.9 cm off for the first data set, and 30 cm to 46 cm for the second. Shifting the results towards the reference points to the nearest reference position, still results in a maximum error of around 18.4 cm for test setup one, and around 16 cm for test setup two. The error is highest for the measured points in the middle and lower for the outer points (Figure 5.6). The distribution of the error can be explained

using the slack, which is biggest in the middle of the cableway and smallest at the beginning and the end.

Furthermore, the calculation is done using the raw height values for each position rather than the mean, to generate 20 solution per position. Figure 5.7 shows the error distribution of these results . The dots in Figure 5.7 represent the mean error, whereas the lines show the 95 % quantile of the error at each position. Again, higher error values for the positions in the middle of the cableway and lower error values for the outer positions can be observed. The 75 % quantile of all error values is 38.2 cm for data set one and 43.3 cm for data set two (Table 5.3). Even after a calibration, the values for the 75% quantile exceed 10 cm. It is noticeable that the average standard deviation per position for test setup two is with 1.06 cm significantly higher than for test setup one. There, an average standard deviation per position of 0.785 cm was determined. The higher variation of the result for the second data set can be explained with the smaller ascent of the cableway used during recording. Therefore, the error of the measured height by the distance sensor of the gondola has a bigger impact on the solution.

Overall, it can be concluded, that the assumption of the rope being a straight line is not suitable to calculate the position of the gondola.

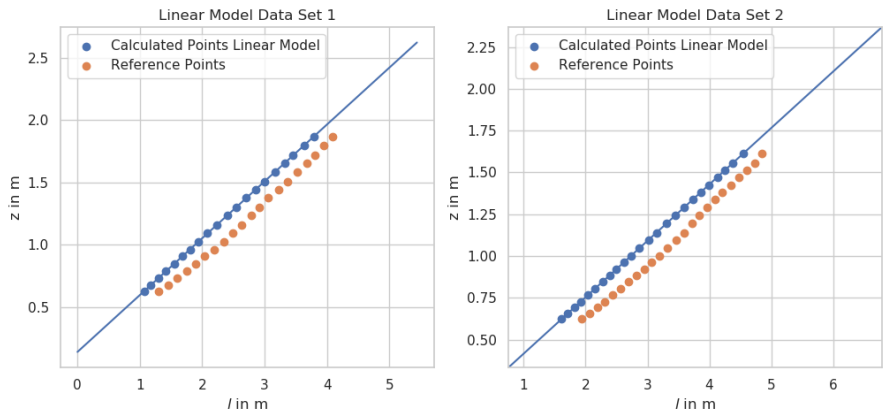

Figure 5.6: Positions Linear Approach

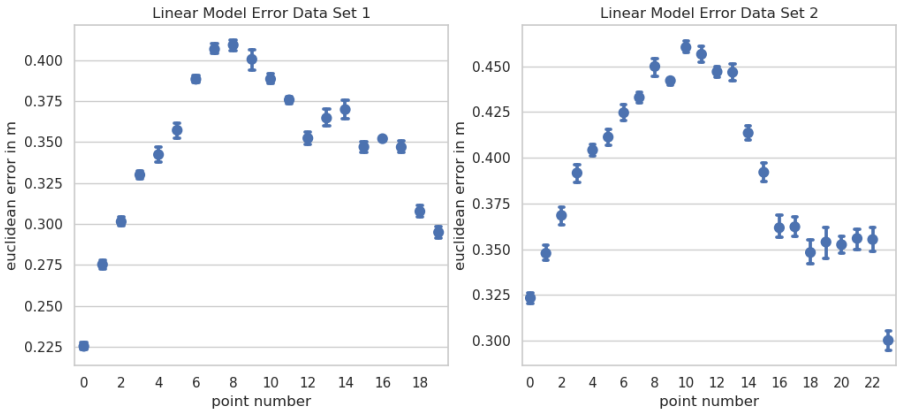

Figure 5.7: Error Distribution Linear Approach

Error	Linear Model		Step Count Model		Slack Model**	
	Setup1	Setup2	Setup1	Setup2*	Setup1	Setup2
	[cm]	[cm]	[cm]	[cm]	[cm]	[cm]
Median	35.25	39.31	3.54	1.27	1.57	4.24
75 % quantile	38.20	43.29	3.92	1.90	2.62	5.35
95 % quantile	41.24	46.02	4.71	2.77	4.82	6.86
IQR	5.92	7.93	1.00	1.25	2.07	2.45
Mean Std p.P.	0.78	1.06	0.19	0.13	0.64	1.07

* results after calibration

** best result for s used (in terms of 95 % quantile error)

Table 5.3: Euklidean Error for Each Model

5.6 Evaluation of the Nonlinear Model: Step Count Method

In this section, in addition to the height, the recorded motor steps are used to calculate the position of the gondola. The steps can be converted to the distance the gondola moved along the cableway at which one step equals a 0.0269 mm movement. By subtracting the distance the gondola is pulled upwards from the measured distance l_{thome}, l_t is calculated. As in the approach

evaluated above, the measured height is increased by the height of the gondola to calculate the point where the gondola is connected to the track rope of the cable car. Also, the height of the anchor point P_{l1} and P_{l2} respectively is considered.

Figure 5.8 shows the results of the calculated positions compared to the reference positions in a 2-dimensional representation. To calculate the positions the recorded motor steps and the mean recorded height for each position is used. The reference positions are the same as in Section 5.5. Again, due to the use of the same height for both the reference positions and the calculations the error for this calculation is only in l and equals the euclidean error in the 3-dimensional representation of the positions. The error between the positions calculated in this approach and the reference positions is between 2.13 cm and 4.74 cm for the first data set. However, for the second data set this error is between 1.62 m and 1.77 m. It can be observed that all calculated positions for the second setup are shifted to the right compared to the reference positions. This can be caused by a faulty measured distance l_{thome2}, probably caused by disturbance of the laser distance measurement tool, or simply human error. Also, the measured distance l_{thome2} is smaller than l_{thome1} even though the second cableway setup is longer. Therefore l_{thome2} should be longer as well, which also indicates a fault during the measurement. By adjusting this value from 4.48 m to 5.98 m, the error is reduced to a maximum of 2.9 cm. A similar but less drastic shift of around 2 cm can be observed for the first data set.

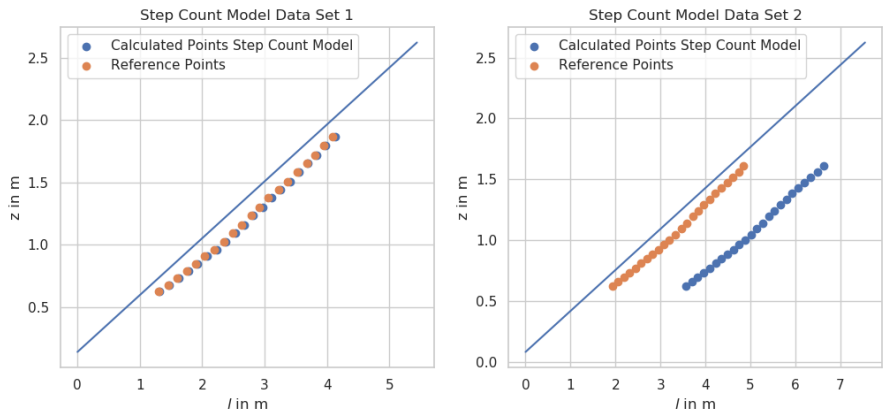

Figure 5.8: Positions Step Count Approach

To evaluate the influence of the variation in the height obtained by the distance sensor the calculation above is repeated using the raw height (no average filtering). Therefore, for each position the gondola drove to during the experiment, 20 solutions are calculated. For the calculations the measured distance l_{thome1} is used for the first data set while the calculations on the second data set use the calibrated value of 5.98 m. Furthermore, the euclidean error of the solutions for each position compared to the measured reference position is calculated. Figure 5.9 shows the distribution of the error for each position. As in Section 5.5, the points in this figure represent the mean error, while the lines show the 95 % quantile.

The mean standard deviation per position (Table 5.3) is 0.19 cm for setup one, and 0.13 cm for setup two, which is less than a third of the standard deviation of the homing procedure and the linear approach. The reason for this is, that the solution also depends on the step count of the motor (l_t) and does not only rely on the measured height. However, the homing procedure and the straight line approach do. Therefore the impact of the height is smaller and so is its measurement error. Additionally, the step count of the motor does not change once the gondola reaches a position. Because all the data was recorded while the cable car was standing still this is always the case during these calculations.

Table 5.3 furthermore shows that the overall error of this method is much smaller compared to the linear approach. Due to the calibration of l_{thome} for setup two, the error of the calculated positions is again smaller than the results for setup one.

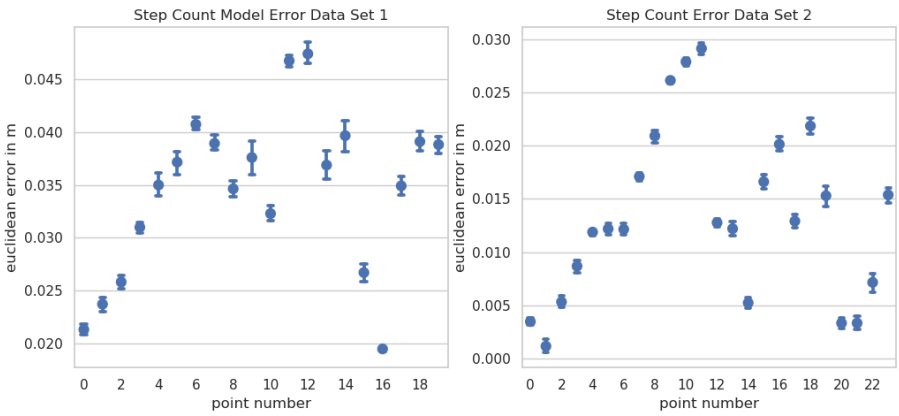

Figure 5.9: Error Step Count Approach

In summary the results show that using the step count of the motor pulling up the gondola in addition to the height sensor enables a compensation of the slack of the cableway. A positioning accuracy of well below 5 cm can be reached.

The error model is approached using a normal distribution for the height and the distance l. To train the model a leave-one-out cross-validation is used on both data sets independently. Therefore, each position with its 20 solutions is seen as a set. For training the error model of the first data set, 19 sets are used with one set left for validation. 23 training sets with again one validation set are used for the second error model trained on the second data set.

Normal Distribution		Setup 1	Setup 2
Height	Mean	0 cm	0 cm
	Std	0.3674 cm	0.3675 cm
	Training Error Mean	0 cm	0 cm
	Training Error Std	0.1081 cm	0.0853 cm
Distance l	Mean	3.4391 cm	1.3133 cm
	Std	0.1944 cm	0.1363 cm
	Training Error Mean	0.6351 cm	0.6889 cm
	Training Error Std	0.0586 cm	0.0323 cm

Table 5.4: Error Model Step Count Method

Table 5.4 shows the trained parameters for the normal distribution and the according training errors. The mean error in height is zero because the reference positions also use the mean height. For the training of the error model for the second test setup the calibrated calculation results are used. This results in a smaller mean error for the second test setup. Figure 5.10 shows points generated using the trained error models to visualize the distribution of the results. 1000 points were generated for each model. Again, due to the calibration for the second data set the results of it are closer to the reference positions and do not have an offset. The overall distribution of the calculated positions is similar for both data sets.

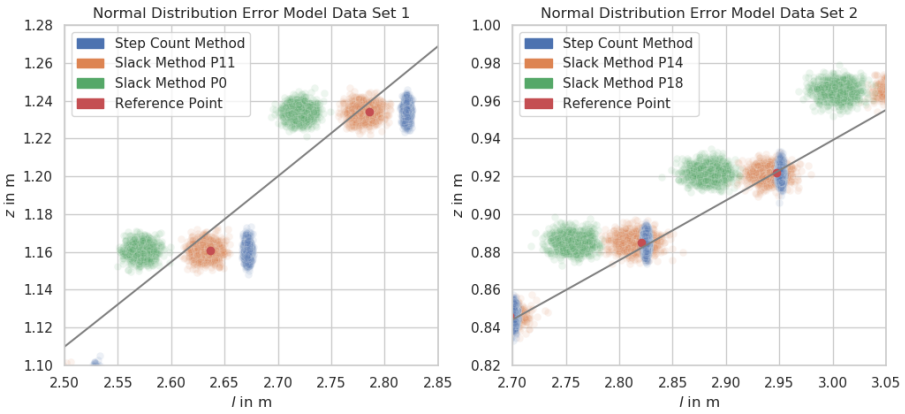

Figure 5.10: Error Model Step Count and Slack Approach

5.7 Evaluation of the Nonlinear Model: Slack Method

In this approach, a curve on which the gondola moved is calculated (Section 4.3). The measured height is then used to get a specific position on this function. First, the rope tension is calculated using the slack of the cableway. To calculate the slack, the height of a reference position is subtracted from the height of its vertical projection onto the a straight line from P_l to P_h. Once the rope tension is known, the slack function over the cableway is calculated. Subtracting the slack function from the linear function from P_l to P_h, the path describing the gondola movement is calculated. To then gain specific solutions for a position of the cable car the measured height of the distance sensor in the gondola is used to get a position on the path. To do so, a simple algorithm is used, which fits the height onto the path to get a position. As in the experiments above, the height of P_l is considered during the calculations and the positions of the gondola calculated equal the connection of the carabiner onto the track rope. Furthermore, the reference positions are again determined by using the mean measured height of the gondola and the manually measured distances.

Figure 5.11 shows the calculated function using reference point 10 in each data set to obtain the rope tension s. For the first test setup this results in a maximum error of 6.62 cm using the mean height to calculate a position on

the curve, and 7.05 cm using the raw height. However, on data set two the maximum error is 14.4 cm using the raw height during calculations, which is more than two times the error of data set one.

The distribution of the results for the first setup in Figure 5.12 indicates that point 0 is a outlier. Again, the dots represent the mean error while the lines show the 95 % quantile. However, this outlier is not visible using the step count based approach because of its different calculation method. Excluding point 0 results in an accuracy of below 5 cm for the first setup, which is similar to the step count based approach. Until point 13, the error for data set two is also always below 5cm. Eventually the results are shifted upwards about 4 cm for the following positions. This indicates that the calculated function only fits the first 15 points. In Figure 5.11 the upper reference points for the second data set are slightly shifted upwards. This can be caused by the light based distance sensor build into the gondola. Different lighting conditions or ground structures with different reflection properties could cause an increased height measured for the last positions. This would result in an error of the reference points. However, due to the systematic error of also using the data of the height sensor for the reference positions and for the different calculation approaches, this error does not appear using the step count based approach.

The performance of the slack approach also depends on the reference point chosen to calculate the rope tension s. Figure 5.13 shows the median error, the 75 % and the 95 % quantile of the error for each reference point used to calculate the rope tension. The overly high error using point 0 in data set one to calculate the rope tension confirms it as an outlier. The best points in terms of the 95 % quantile error are point 11 for data set one with 4.82 cm, and point 14 for data set two with 6.86 cm. Using the mean rope tension overall reference points results in a 95 % quantile error of 5.15 cm for the first test setup, and 6.94 cm for the second, which is in both cases is just slightly bigger than the best results achieved. There is no tendency towards inner or outer points achiving better results. For further comparisons, the rope tension is calculated with the points with the lowest 95 % quantile error for each setup (point 11 and 14). The 95 % quantile describes the performance of the system more accurate than the 75 % quantile and still sorts out outliers.

Table 5.3 shows the overall performance of all three proposed methods for both test setups. The results of the second test setup are worse than the results for the first, using the slack model. The standard deviation for the slack method

is quite similar to the values of the linear model. Both methods use only the height to find a position on a path. Also, as for the linear model, the mean standard deviation per position is higher for the second setup due to its smaller slope and the therefore higher impact of errors of the height sensor. While the slack model outperforms the non-calibrated step count model in accuracy for test setup one, it can not compete with the calibrated step count model in test setup two.

Normal Distribution		Setup 1	Setup 2
Height	Mean	0 cm	0 cm
	Std	0.3674 cm	0.3675 cm
	Training Error Mean	0 cm	0 cm
	Training Error Std	0.1081 cm	0.0853 cm
Distance l	Mean	-0.4705 cm	-0.6466 cm
	Std	0.8128 cm	1.1079 cm
	Training Error Mean	1.6375 cm	4.1980 cm
	Training Error Std	0.2405 cm	0.2376 cm

Table 5.5: Error Model Slack Method

Overall, this method to calculate the position of the gondola manages to generate results with a maximum error of less than 10 cm and a 95 % quantile error of less than 7 cm. Even though the calibrated step count based approach outperforms this method, especially in the variation of the results, it is still suitable to calculate a position of the cableway, with the advantage of not needing a step count capable winch. As for the step count based approach the error model of this method is approached using a normal distribution for the height and the distance l. Also, a leave-one-out cross-validation is used with 19 training sets and one validation set on recorded data set one and 23 training sets and again one validation set on recorded data set two. Table 5.5 shows the results of the trained normal distributions and the training error for each parameter. The error models in Table 5.5 are based on the results gained by using reference point 11 for test setup one, and reference point 14 for setup two to calculate the rope tension s. The height error is the same as for the method above, since the same data is used. Figure 5.10 shows the determined error models by generating 1000 points using the particular model. It can be

seen, that the not calibrated step count method is shifted to the right, while the slack method using point 11 fits the reference point on the first data set. Furthermore, it visualizes that the variation of the results are higher for the slack method. For test setup two the step count method matches the reference point more precisely than the slack method does. Furthermore, the error model using point 0 for test setup one and 18 for test setup two is plotted the same way as mentioned above. Both results show the impact of choosing a not suitable reference point to calculate the slack, which mainly results in a shift. The error models which use a worse fitting point to calculate the rope tension s also come with a higher training error. This shows that both approaches to calculate the position of the gondola benefit from a calibration.

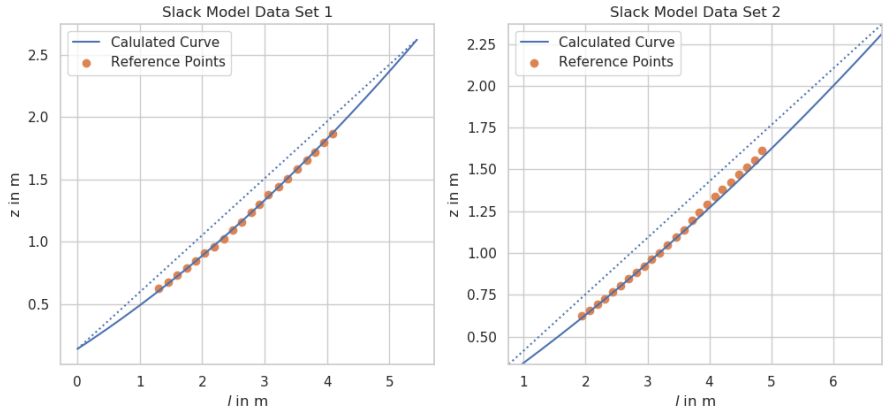

Figure 5.11: Positions Calculated Slack Approach (Point 10)

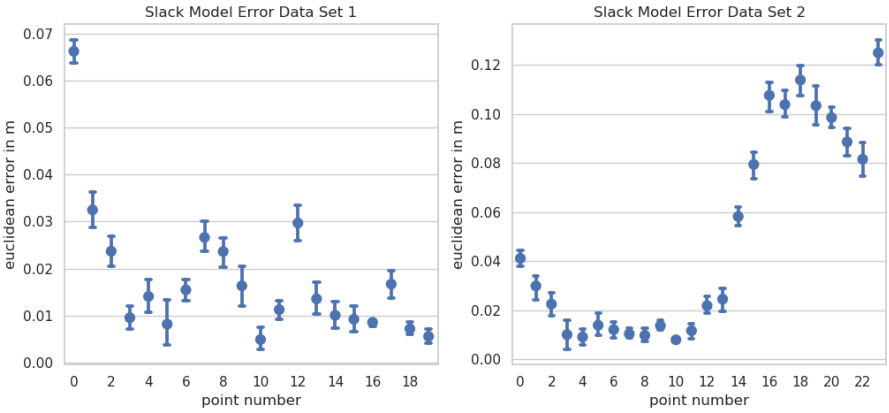

Figure 5.12: Euclidean Error Slack Approach (Point 10)

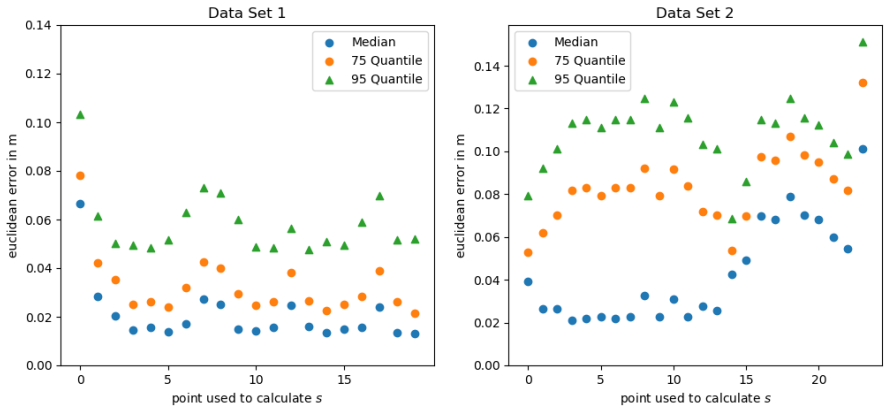

Figure 5.13: Euclidean Error Slack Method with Different Rope Tensions

5.8 Evaluation of the Ultra Wide Band Localization System

In this chapter, the test setup is used to perform a rough analysis of the installed DWM1000 based ultra wide band localization system. Based on the logged distances generated by the DWM1000 modules, a position is calculated using a simple iterative gradient solver. To enable a comparison between the position calculated by the ultra wide band system and the cableway positions, the cableway positions of the gondola are adjusted to fit the position of the antenna of the DWM1000 module mounted to the gondola, rather than the connection of the carabiner to the track rope. In this chapter only the adjusted cableway positions are used. The position of the DWM1000 module at the gondola is as the gondola itself based on the quadrocopters [31] which are used in the laboratory where the DWM1000 based localization system is installed in. In the future, the quadrocopters of the lab are going to use those modules to locate themselves within the room. This section aims to give an overview, whether it is possible to use the setup for localization of the drones or not. Furthermore the suitability of the calculation methods for the cableway positions as reference are evaluated.

Before actual positions are compared the measured reference positions are used to calculate distances to the nine DWM1000 anchor nodes. Eventually, these distances are compared to the ones gained through the two way ranging.

The mean euclidean error for each distance is between 13.4 cm and 24.5 cm for the first setup of the cableway and between 10.8 cm and 51.5 cm for the second. The worst fitting distances of each setup do not belong to the same anchor point. That indicates that the reason for the high errors is not a faulty measured position of an anchor node. The 75 % quantile of the error over all distances is 22.98 cm for the first and 36.27 cm for the second data set. For the second setup the error of the distances is noticeably higher than for the first.

The mean position error between the calculated position and the adjusted reference position using the first setup of the cableway is 29.5 cm and 51.3 cm using the second setup. Noticeable is that in both setups the solutions generated by the ultra wide band localization system are shifted away from the actual points in the direction the localized module is mounted on the gondola (Figure 5.14). The shift of the results can be explained by assuming that the gondola blocks signals and thereby influences the distances measured, so that anchors with no direct line of sight are reporting higher distances. This would shift the results away from the anchors with no line of sight, where the gondola is between the DWM1000 module mounted to it and the anchor node. To verify the assumption above the gondola first was placed with its module facing towards an anchor node and then facing away, each time with a distance of 80 cm from module to module (Figure 5.16). Over one hundred measurements the distance generated with the module facing towards the anchor node, is between 0.93 m and 1.01 m, whereas the distance generated with the module facing away from the anchor node, so that the gondola is in between direct line of sight, results in 1.26 m to 1.35 m. That can be used not only to explain the offset but also to explain the overall higher error for the second cable way setup. There, the DWM1000 module mounted on the gondola was facing away from more DWM1000 anchor nodes than during the first setup. Therefore, the overall error in the measured distances, and through that the resulting position is worse. The experiment furthermore shows that even with line of sight, the measured distance is more than 10 cm higher than the actual distance of 80 cm.

Next, the different calculations approaches for the cableway positions are compared. For each calculation approach the error of the gradient solver solutions to the particular approach are calculated. These errors are then compared to the error calculated above, using the measured reference points. That way, Figure 5.15 shows the impact of using a certain method to calculate the gon-

dola points rather than using the measured points to analyze the error of the installed ultra wide band localization system. The dots represent the median error, while the lines show the 95 % quantile of the difference. The linear calculation method is left out since the 75 % quantile of the difference is around 30 cm for the first and 35 cm for the second data set. This again shows that this method is not suitable to calculate the position of the gondola. However, there is only a very small difference in using the other two calculation methos to analyze the ultra winde band localization system instad of using the measured points. The 95 % quantile of the difference is slightly smaller for the slack method with around 2.5 cm during the first setup than for the step count method with around 3 cm. Nevertheless, for the second setup the step count based calculation approach competes with around 2 cm as 95 % quantile against the slack based approach with around 5 cm. Still, both approaches are appropriate to compare against the installed ultra wide band localization system.

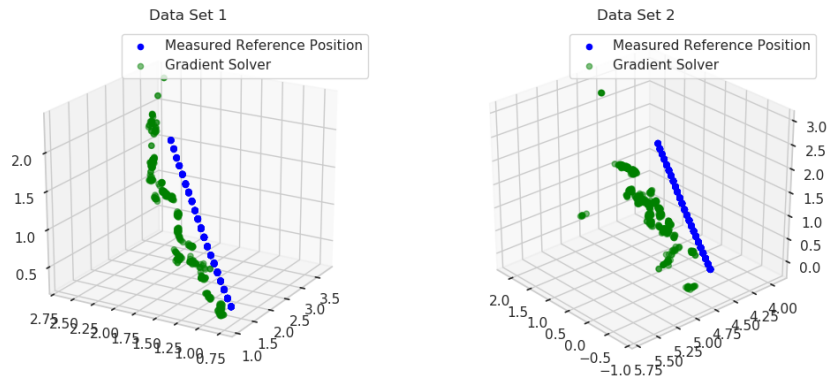

Figure 5.14: Reference and Ultra Wide Band Localization Positions

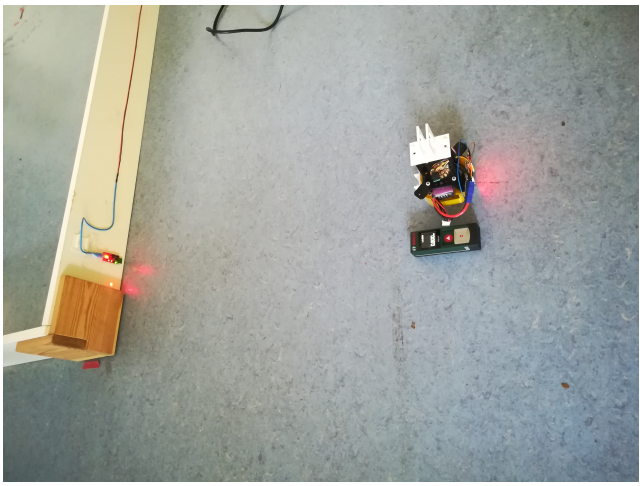

Figure 5.16: Distance Measured with Gondola Blocking Line of Sight

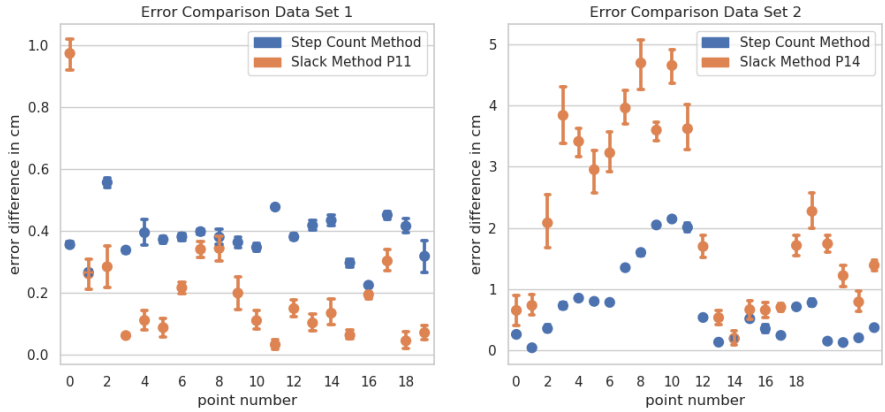

Figure 5.15: Error Comparison of Different Calculation Approaches

5.9 Summary

In this chapter, the three different proposed methods to calculate the position of the gondola were evaluated. The results show that the linear approach is not suitable to do so for the purpose in this thesis. Furthermore, the results of the slack based approach and the step count based approach show similar performance of the two methods in therms of accuracy. However, the variation of the results is much smaller for the step count method. Instead, the slack

method comes with the advantage of not needing a motorized winch capable of counting steps. In the end, it is shown that the cableway is suitable to be used as a ground truth for the installed ultra wide band localization system.

6 Conclusion

In this work, a cableway is used as 3-dimensional ground truth for indoor localization systems.

The installed cableway describes a trajectory trough 3-dimensional space and enables the gondola to move to any position on that path. Through the use of different anchor points of the cableway the trajectory can be changed. The path of the gondola can also be adjusted by changing the tension within the track rope. Therefore, the cableway is capable of generating various reference positions in 3-dimensional space.

To calculate the position of the gondola, three different methods were used. The results show that the step count based approach is able to calculate a position with 95 % of the error below 5 cm. Similar results are achievable with the slack based approach (Table 5.3). In terms of variation of the results however, the step count method clearly outperforms the other two approaches. The results furthermore show that the linear approach is not appropriate to calculate the position of the gondola.

For the step count based and the slack based approach an error model is trained, as these are the best methods. It turns out that a normal distribution is sufficient to describe the results.

Overall, an accuracy of well below 10 cm can be reached using the slack based and the step count based approach. The slack method is slightly less accurate than the step count method but comes with the advantage of a much simpler setup since it does not need a motorized winch to work.

Another requirement for the constructed ground truth is an easy and flexible setup. The cableway can easily be reinstalled at a different location by simply mounting the track rope at two known points in a room. Depending on the method to calculate the position of the gondola, either the distance l_t, or one reference point needs to be measured to use the ground truth. In addition

the proposed system enables a flexible use for different localization systems, since the gondola is reconfigurable. For instance, a marker could easily be attached to the gondola, making the ground truth usable for an optical system. Therefore, the ground truth offers an easy installation and a flexible use.

The cableway was constructed with a budget of less than 200 euro. The investments done consist of a stepper motor, a pulley and some climbing gear. The height sensor, battery and ranging modules were components used by the drones of the laboratory and therefore came at no cost. Furthermore, 3d printed parts were used to construct the winch and pieces of the cable car. Even if the cost of the whole setup might be over 200 euro, the actual parts bought for the assembly barely reached the 100 euro mark.

In the end, an ultra wide band localization system, to be used for drones, has been considered. The results show that the system is currently not precise enough to be used to localize drones due to falsely measured distances from the localized module to the anchor nodes. Better performance of the system can be achieved by better placement of the tracked module to enable line of sight to as many anchor nodes as possible. Furthermore, the cableway itself turns out to be an appropriate ground truth to analyze and calibrate the system.

In this work, a flexible, easy to install ground truth, which enables 3-dimensional positioning within an 95 % accuracy of below 5 cm at low cost, is introduced. The constructed cableway thereby fulfills all requirements set (Section 1.2) and can be used as a ground truth for indoor positioning systems.

7 Future Work

This chapter suggest further work based on the ground truth proposed in this thesis.

The accuracy of the proposed test system is mainly based on the used height sensor. By evaluating different sensors, the performance of the cableway could be improved. Also, the path of the cableway only goes upwards, so the height sensor can be used to determine a position on the cableway. The smaller the ascent of the cableway, the higher is the influence of the height sensors error. Therefore, the length of the cableway itself is limited. By combining the slack method with the step count based approach, a cableway as ground truth with two anchor points at the same height could be built. This would not only increase the possible length of the setup but also could improve the overall accuracy.

Furthermore, the cable car can be used to improve the installed ultra wide band localization system. Therefore, the partially coverage of the antenna needs to be change to enable line of sight to more anchor nodes.

In addition, different algorithms can be tested. For instance, an implementation based on choosing suitable anchors rather than using all ranging results to determine a position using the DWM1000 based system could be evaluated. Also, the influence of different DWM1000 anchor positions remains to be analyzed.

In the end, the ground truth can be used to compare results of different configurations of the installed ultra wide band localization system.

Bibliography

[1] AltBeacon - The Open Proximity Beacon. https://altbeacon.org/. Accessed: 2019-06-05.

[2] angle-of-arrival an overview | ScienceDirect Topics. https://www.sciencedirect.com/topics/engineering/angle-of-arrival. Accessed: 2019-06-25.

[3] Avvel X Beacon - 100m iBeacon - Amazon.co.uk.

[4] Datasheet laser distance sensor LDS-01. http://emanual.robotis.com/docs/en/platform/turtlebot3/appendix_lds_01/. Accessed: 2019-06-03.

[5] Estimote indoor location with bluetooth beacons and mesh. http://estimote.com/. Accessed: 2019-06-05.

[6] The Implementation of Two Way Ranging with the DW1000 - APS013 Application Note Version 2.3.

[7] Indoor Positionsbestimmung - Basisinformationen von infsoft. https://www.infsoft.com/de/indoor-positionsbestimmung. Accessed: 2019-04-02.

[8] OptiTrack System Configurator. http://www.optitrack.com/systems/index.html. Accessed: 2019-04-17.

[9] Robotis TURTLEBOT3 Burger. https://www.mybotshop.de/ROBOTIS-TURTLEBOT3-Burger_1. Accessed: 2019-06-03.

[10] Stepper motor driver library | Mbed. https://os.mbed.com/users/melse/code/StepperMotor/. Accessed: 2019-03-05.

[11] TeraRanger One distance sensor. https://www.terabee.com/shop/lidar-tof-range-finders/teraranger-one/. Accessed: 2019-06-25.

[12] Seilstatik, Kettenlinien, Stützlinien. In Jürgen Dankert and Helga Dankert, editors, *Technische Mechanik: Statik, Festigkeitslehre, Kinematik/Kinetik*, pages 143–152. Teubner, Wiesbaden, 2006.

[13] Robotic Mapping: Simultaneous Localization and Mapping (SLAM). `https://www.gislounge.com/robotic-mapping-simultaneous-localization-and-mapping-slam/`, January 2013. Accessed: 2019-07-09.

[14] Accurate indoor positioning with Bluetooth beacons. `https://proximi.io/accurate-indoor-positioning-bluetooth-beacons/`, July 2017. Accessed: 2019-06-05.

[15] Anja Bekkelien. Bluetooth indoor positioning, March 2012.

[16] Jan Dyre Bjerknes, Wenguo Liu, Alan FT Winfield, and Chris Melhuish. Low Cost Ultrasonic Positioning System for Mobile Robots.

[17] BOSCH. Laser distance meter PLR15 User Manual.

[18] F. Serhan Daniş and Ali Taylan Cemgil. Model-Based Localization and Tracking Using Bluetooth Low-Energy Beacons. *Sensors (Basel, Switzerland)*, October 2017.

[19] S. De Amici, A. Sanna, F. Lamberti, and B. Pralio. A Wii remote-based infrared-optical tracking system. *Entertainment Computing*, 1(3):119–124, December 2010.

[20] Decawave. DWM1000 Module - Product Page. `https://www.decawave.com/product/dwm1000-module/`. Accessed: 2019-06-25.

[21] Markus Hempel. Programming and Evaluation of an Ultra-Wideband Distance Measurement System for Mobile Robots. page 77.

[22] Stemmer Imaging. 3d Time of Flight-Kameras Grundlagen. `https://www.stemmer-imaging.com/de-de/grundlagen/kameras-3d-time-of-flight-kameras/`. Accessed: 2019-06-25.

[23] ITWissen.info. AoA (angle of arrival) - Einfallswinkel. `https://www.itwissen.info/AoA-angle-of-arrival-Einfallswinkel.html`. Accessed: 2019-06-25.

[24] ITWissen.info. Empfangsfeldstärke RSS (received signal strength). `https://www.itwissen.info/`

Empfangsfeldstaerke-received-signal-strength-RSS.html. Accessed: 2019-06-25.

[25] Benjamin Kempke, Pat Pannuto, and Prabal Dutta. PolyPoint: Guiding Indoor Quadrotors with Ultra-Wideband Localization. In *Proceedings of the 2nd International Workshop on Hot Topics in Wireless - HotWireless '15*, pages 16–20, Paris, France, 2015. ACM Press.

[26] Jiří Kárník and Jakub Streit. Summary of available indoor location techniques, 2016.

[27] Minghui Li and Yilong Lu. Angle-of-arrival estimation for localization and communication in wireless networks. *European Signal Processing Conference*, January 2008.

[28] Alberto Lopez-Ceron, Universidad Rey Juan Carlos, Jose M Canas, and Universidad Rey Juan Carlos. Accuracy analysis of marker-based 3d visual localization.

[29] Sebastian Mai. Board to interface the DWM1000 Decawave-Module with a STM32l443cc microcontroller: bastinat0r/DWM-1000-Adapter-board. https://github.com/bastinat0r/DWM-1000-Adapter-board, May 2018. Accessed: 2019-06-25.

[30] Rainer Mautz and Sebastian Tilch. Survey of optical indoor positioning systems. In *2011 International Conference on Indoor Positioning and Indoor Navigation*, pages 1–7, Guimaraes, Portugal, September 2011. IEEE.

[31] Chair of Computational Intelligence Magdeburg. FINken Drones. https://www.is.ovgu.de/SwarmLab/Robots/FINkens.html. Accessed: 2019-07-09.

[32] Brian O'Keefe. Finding Location with Time of Arrival and Time Difference of Arrival Techniques. page 3.

[33] Jun Qi and Guo-Ping Liu. A Robust High-Accuracy Ultrasound Indoor Positioning System Based on a Wireless Sensor Network. *Sensors (Basel, Switzerland)*, 17(11), November 2017.

[34] simekmilan. Two Way Ranging (TWR). https://www.sewio.net/uwb-technology/two-way-ranging/. Accessed: 2019-07-02.

[35] TERABEE. TeraRanger One Manual V1.0.

[36] Janis Tiemann, Florian Schweikowski, and Christian Wietfeld. Design of an UWB indoor-positioning system for UAV navigation in GNSS-denied environments. In *2015 International Conference on Indoor Positioning and Indoor Navigation (IPIN)*, pages 1–7, Banff, AB, Canada, October 2015. IEEE.

[37] WELT. Amazon: Lieferung per Drohne startet in wenigen Monaten. June 2019.

[38] C. Yang and H. Shao. WiFi-based indoor positioning. *IEEE Communications Magazine*, 53(3):150–157, March 2015.

[39] Ugur Yayan, Hikmet Yucel, and Ahmet Yazıcı. A Low Cost Ultrasonic Based Positioning System for the Indoor Navigation of Mobile Robots. *Journal of Intelligent & Robotic Systems*, 78(3):541–552, June 2015.

Declaration of Authorship

I hereby declare that this thesis was created by me and me alone using only the stated sources and tools.

Jonathan Beckhaus Magdeburg, 17.07.19